OBSERVATIONS OF LUNAR SWIRLS BY THE DIVINER LUNAR RADIOMETER EXPERIMENT. T. D. Glotch[1], B. T. Greenhagen[2], P. G. Lucey[3], J. L. Bandfield[4], Paul O. Hayne[5], Carlton C. Allen[6], Richard C. Elphic[7], and D. A. Paige[8], [1]Department of Geosciences, Stony Brook University, tglotch@notes.cc.sunysb.edu, [2]Jet Propulsion Laboratory, [3]Hawaii Institute of Geophysics and Planetology, University of Hawaii, [4]University of Washington, [5]California Institute of Technology, [6]NASA Johnson Space Center, [7]NASA Ames Research Center, [8]University of California at Los Angeles.

Introduction: The presence of anomalous, high albedo markings on the lunar surface has been known since the Apollo era [1]. These features, collectively known as lunar swirls, occur on both the mare and highlands. Some swirls are associated with the antipodes of major impact basins, while all are associated with magnetic field anomalies of varying strength [2-3]. Three mechanisms have been proposed for the formation of the swirls: (1) solar wind standoff due to the presence of magnetic fields [4], (2) micrometeoroid or comet swarms impacting and disturbing the lunar surface, revealing unweathered regolith [5-6], and (3) transport and deposition of fine-grained feldspathic material [7].

Diviner's unique capabilities to determine silicate composition and degree of space weathering of the lunar surface [8-10], in addition to its capabilities to determine thermophysical properties from night-time temperature measurements [11], make it an ideal instrument to examine the swirls and help differentiate among the three proposed formation mechanisms.

Data and Methods: Diviner daytime data were acquired between 10:00 am and 2:00 pm local solar time with emission angles < 12.5°. Daytime data were binned at 128 ppd using a topographic model and converted to emissivity [12]. The emissivity data were then used to determine the position of the Christiansen Feature (CF) according to the method of [9]. The wavelength position of the CF, which is dependent on the degree of polymerization, has been shown to be a good compositional indicator for silicate minerals [13-14], and has been used to map silicate compositional differences on the Moon [9]. Diviner channel 8 (50-100 μm) night-time data were collected between 7:30 pm and 5:30 am and binned at 128 ppd. For each 1 hour increment between these times, the temperature deviation from the scene average was used to create a temperature image.

Results: We have collected and binned daytime and night-time data for the Reiner Gamma, Airy, Mare Ingenii, and Mare Marginis swirls. For each region, a Diviner CF anomaly is observed for the high-albedo swirl relative to the immediate background. Figure 1 shows a Diviner CF map overlayed on an LROC WAC mosaic covering the central region of the Reiner Gamma swirl. The blue region of the map, representing low CF values, corresponds directly to the high-albedo regions of the swirl. Corresponding Diviner 3-point spectra acquired on and off the swirl are shown in Figure 2.

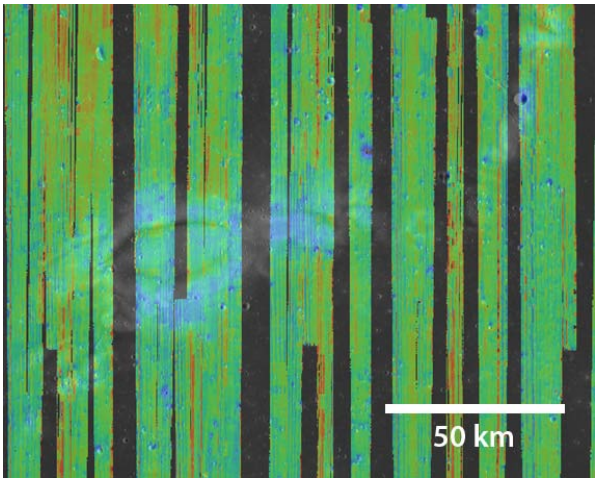

Figure 1. Diviner CF map covering the central portion of Reiner Gamma overlain on a LROC WAC mosaic. The CF map is stretched from 8.1 (blue) to 8.5 μm (red) and clearly shows an anomaly related to the high albedo portion of the Reiner Gamma swirl.

Night-time Diviner data covering the same region of the Reiner Gamma swirl are shown in Figure 3. There is not a substantial anomaly associated with the swirl, as temperatures on the swirl are only ~1 K colder than the surrounding terrain. The major temperature deviations present in the night-time data are related to the presence of small craters in the region, typical of

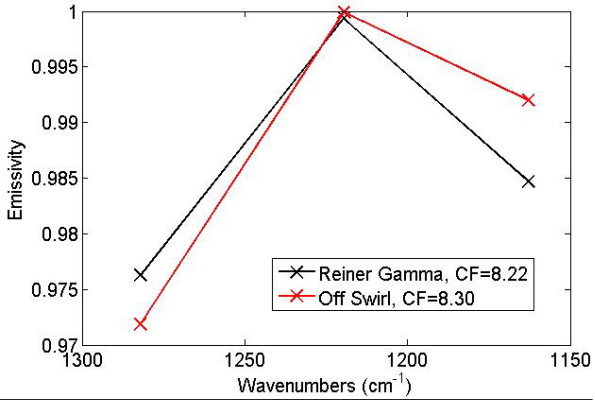

Figure 2. Average emissivity spectra of the central portion of the Reiner Gamma swirl and nearby low-albedo background.

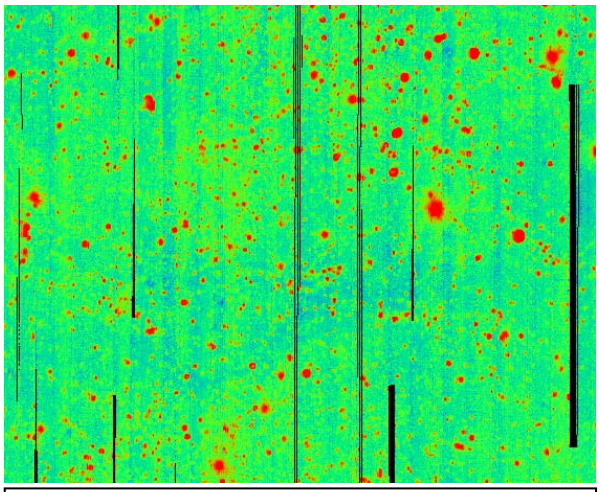

Figure 3. Diviner night-time temperature map covering the region shown in Figure 1. The image is stretched from -12 to +12 ΔK. Little if any temperature anomaly is associated with the Reiner Gamma swirl.

lunar maria.

Both the daytime and night-time characteristics described for the Reiner Gamma swirl hold for the other three swirls that we have examined thus far. CF anomalies range from -0.03 to -0.12 μm and temperature anomalies range from -1.1 to +0.5 K.

Discussion: Diviner observations of the lunar swirls are generally consistent with the proposed solar wind standoff formation mechanism. In each case the observed CF position is shifted a small amount to shorter wavelengths compared to the immediate background. This is consistent with the observation that space weathered surfaces tend to have CF positions that are shifted to slightly longer wavelengths compared to optically immature surfaces of the same composition [10]. Standoff of solar wind at the swirls is also supported by M^3 observations that show a lack of OH formation at the swirls [15].

Garrick-Bethel et al. [7] proposed that the swirls form as a result of deposition of fine-grained plagioclase-rich dust that are transported by electric fields along the terminator. There are two lines of evidence suggesting this hypothesis is not correct. The first is the observed CF positions of the the swirls, which range from 8.18 to 8.30 μm. Anorthositic plagioclase feldspar has a CF position of 7.86 μm [9]. To account for the observed CF positions of the swirls, a substantial portion of mafic material would have to be mixed with the plagioclase, which would lower their albedoes. The second line of evidence disputing the plagioclase dust hypothesis is the lack of a strong night-time thermal anomaly associated with the swirls. A larger low-temperature anomaly would be expected if a substantial accumulation of dust was responsible for the swirls. Diviner's night-time measurements are consistent with data from the Mini-RF radar that show the swirls to be superficial features [16].

The lack of substantial thermal anomalies associated with the swirls also conflicts with the micrometeorioid/comet swarm impact hypothesis. Impacts in general tend to create blocky material with high thermal inertias, as can be seen for the small craters in Figure 3. Even in cases where impactors do not excavate rocks and only disturb the near surface regolith, significant night-time temperature anomalies would be expected. Typical lunar regolith is finely structured and any excavation or disturbance of a layer greater than a few mm would be readily detected. In Figure 3, however, the bluish region is only ~ 1 K colder than the surrounding terrain, suggesting such a layer is not present.

Implications for space weathering: As was shown by [10], Diviner data are sensitive to space weathering of the lunar surface. Space weathering is generally considered to be the product of two processes—solar wind sputtering resulting in a patina of nanophase Fe^0 particles, and micrometeorite impacts resulting in agglutinitic glass formation. The magnetic fields associated with the swirls appear to be strong enough to prevent interaction of the solar wind with the surface, but they would not affect bombardment of the surface by micrometeorites. This suggests that at mid-IR wavelengths, like in the VNIR [17]. the optical effects of space weathering are due to the presence of nanophase Fe, and are only weakly, if at all dependent on the presence of agglutinitic glass.

References: [1] El-Baz F. (1972) *NASA SP 315, 29-97*. [2] Hood L. L. and Williams C. R. (1989) *Proc. Lunar Sci. Conf. 19, 99-113*. [3] Richmond N. C. et al. (2005) *J. Geophys. Res.*, 110, E05011. [4] Hood L. L. and Schubert, G. (1980) *Science*, 208, 49-51. [5] Schultz P. and Srnka L. (1980) *Nature*, 284, 22-26. [6] Starukhina L. V. and Shkuratov Y. G. (2004) *Icarus*, 167, 136-147. [7] Garrick-Bethel I. et al. (2011) *Icarus*, 212, 480-492. [8] Glotch T. D. et al. (2010) *Science*, 329, 1510-1513. [9] Greenhagen B. T. et al. (2010) *Science*, 329, 1507-1509. [10] Lucey P. G. et al. (2010) *LPS XLI*, Abstract #1600. [11] Bandfield J. L. et al. (2011) *J. Geophys. Res.*, 116, E00H02. [12] Greenhagen B. T. et al. (2011) LPS XLII, Abstract #2679. [13] Conel J. E. (1969) *J. Geophys. Res*., 74, 1614-1634. [14] Salisbury J. W. and Walter L. S. (1989) *J. Geophys. Res.*, 94, 9192-9202. [15] Kramer G. Y. et al. (2011) *J. Geophys. Res.*, 116, E00G18. [16] Neish C. D. et al. (2011) *Icarus*, 215, 186-196. [17] Pieters et al (2000), MAPS, 35, 1101-1107.